All Sciences Proceedings

1st International Conference on Scientific and Innovative Studies

April 18-20, 2023 : Konya, Turkey

ICSIS

All Sciences Proceedings
http://as-proceeding.com/

https://as-proceeding.com/index.php/icsis

Analysis & Simulation of Different LLC Converter Topologies

Abdel Hadi Daher[1], Nezihe Yıldıran [2*]

[1]Mechatronics Engineering Department/Bahceseehir University, Turkey
[2]Energy Systems Engineering Department/Bahceseehir University, Turkey

[*](nezihe.kucukyildiran@eng.bau.edu.tr) Email of the corresponding author

Abstract **–** There is an expanding trend in electric vehicle (EV) technologies because of finite fuel sources and environmental concerns. One of the essential barriers in EVs commercialization is the charging of batteries. The inductor-inductor-capacitor (LLC) resonant converter appears the most appealing design due to its advantages, such as small electromagnetic interference, obtaining high-power density, ability to be designed at very high switching frequencies, operation for wide input and output voltage range with narrow switching frequency variation, and high efficiency. This study compares different topologies of LLC resonant converter that can be adapted as battery charger of electric vehicle. The schematics of topologies, detailed design calculation of the parameters, simulation results of topologies to show the circuit performance are presented, respectively. The simulation model is realized for whole examined topologies with a proportional integral controller to obtain constant output voltage using MATLAB. LLC resonant circuit is designed for the input voltage range of 305-345V, output voltage range of 36-58V, and output power of 700W. Analytical and simulation results are included in this study to illustrate the performance differences among the presented topologies of LLC resonant converter in terms of structure, efficiency, and dynamic response at sudden load changes.

Keywords – Battery Charger; Electric Vehicle; First Harmonic Approximation; LLC Resonant Converters; PI Controller

I. INTRODUCTION

Electricity has an important role in the economic, social development, and the prosperity of the developed countries. Therefore, electric transportation has received great attention from researchers during the past two decades to reduce fuel consumption by finding alternative sources [1].

Today, electric vehicle (EV) and hybrid electric vehicle (HEV) industry emerge quickly, and gain more marketplace in the automotive industry, motivated mainly by environmental concerns. One of the important challenges in EVs commercialization is battery charging. Various topologies and schemes of DC-DC converters have been proposed and used in EV battery charging to obtain regulated output voltage and current.

In the electric vehicle (EV) battery charger architecture as showing in Fig. 1, a DC-DC converter is a key element. Generally, the battery charger takes the DC link voltage supplied by an AC-DC converter with power factor correction (PFC) circuit and an isolated DC-DC converter charges the batteries [2].

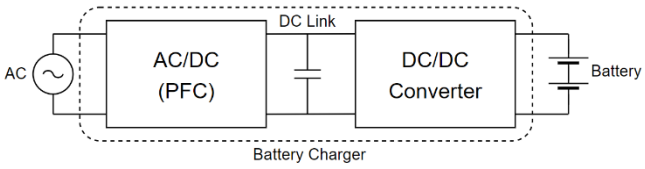

Fig. 1 Block diagram of battery charger

Different LLC resonant converter topologies have been explored in the literature, such as LLC resonant half-bridge converter with center tapped full-wave rectifier [3], LLC resonant half-bridge converter with a full-wave bridge rectifier [4], LLC

resonant full-bridge converter with center tapped full-wave rectifier [5], LLC resonant full-bridge converter with a full-wave bridge rectifier [6]. Recent LLC resonant Full-bridge converter for the EV battery charging proposed and examined which consists of parallel two transformer [7].

Generally, the method used for regulating the output voltage and current is switching frequency modulation in LLC resonant converters. Because of non-linear characteristics of the LLC converters, the predictable performance is difficult to achieve using conventional linear control strategies. A linear proportional integral controller could be integrated to control/adjust the output voltage at specific values [8]. The strategy is to increase the voltage by decreasing the frequency while in case of high voltage output the frequency is reduced. A sudden load condition created for LLC converter using PI controller [9, 10]. A constant output voltage is gained with variation of output current at sudden load. PID (proportion integral differentiation) controller is suggested to improve the dynamic response using the differentiation parts of the PID controller [11]. Even so, it effects the stability of the converter to improve the system damping, current loops and order controller are used [12-14]. There are many proposed intelligent algorithms, but they are too complex to be realized. Such schemes are:

- sliding mode control [15],
- robust control [16],
- self-adaptive fuzzy control [17],
- bang-bang control [18].

In this study, PI controller has been preferred after the comparison of control and complexity equilibrium. The contribution of this paper is comparison of four different LLC resonant converter topologies in terms of structure, efficiency, and dynamic response at sudden load changes with PI controller.

II. Materials and Method

Four different topologies of LLC resonant converter are considered in this study. The topologies are:

- Topology 1: Half-bridge switching network with center tapped full wave rectifier (Fig. 2),
- Topology 2: Half-bridge switching network with full-wave bridge rectifier (Fig. 3),
- Topology 3: Full-bridge switching network with center tapped full-wave rectifier (Fig.4),
- Topology 4: Full-bridge switching network with two transformers network with two full-bridge rectifiers (Fig. 5).

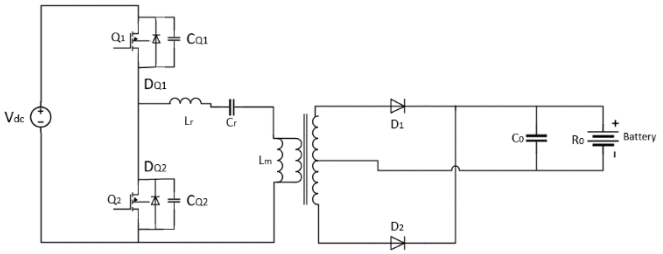

Fig. 2 Topology 1 (T1)

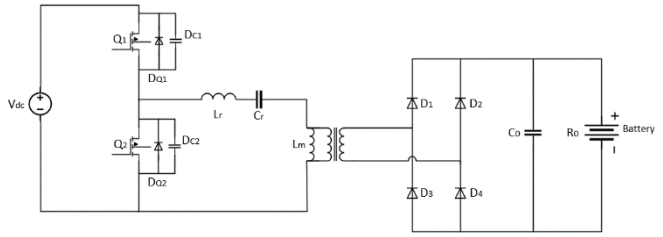

Fig. 3 Topology 2 (T2)

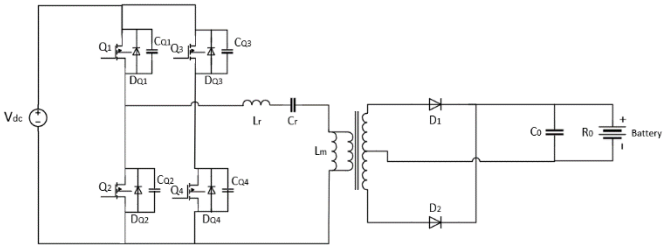

Fig. 4 Topology 3 (T3)

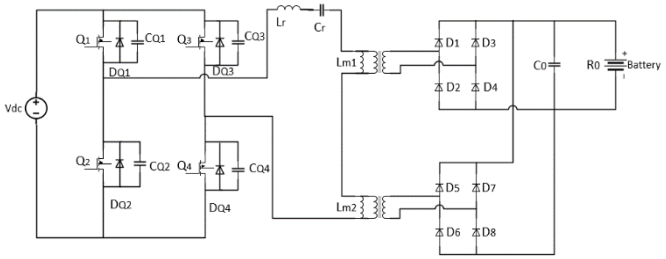

Fig. 5 Topology 4 (T4)

Fig. 4 shows the converter output circuit block. By using first harmonic approximation (FHA) method, as shown in Fig. 6, the LLC converter output circuit can be greatly simplified after approximating the square waves by their fundamental harmonics. The output equivalent circuit of output filter, transformer, rectifier, and load can be replaced by an equivalent resistor which is connected in parallel with L_m. Fig. 7 illustrates the

simplified form of LLC resonant circuit after the first harmonic approximation.

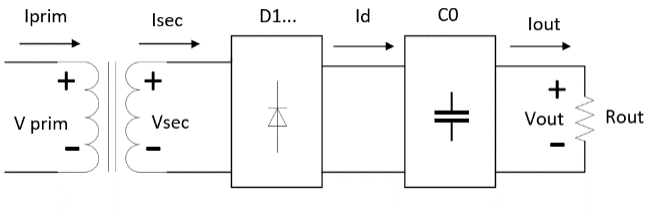

Fig. 6 Converter output circuit

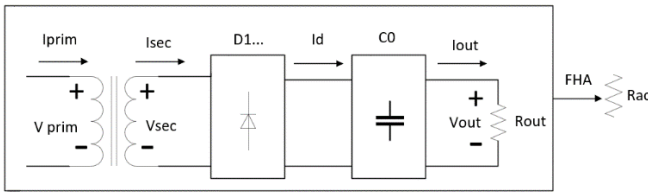

Fig. 7 FHA approximation of the output circuit

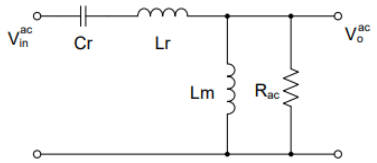

Fig. 7 Simplified form of LLC circuit after FHA

III. RESULTS

The simulation of various type of LLC resonant converter designed to charge batteries with maximum output power of 700W. The input voltage is 305-345V with the nominal voltage of 325V: The charger output voltage is 36-58V with the nominal voltage of 48V. The resonant frequency is 100 kHz. The flowchart of design procedure is given in Fig. 8. The parameters are determined for each topology and the values are summarized in Table 1.

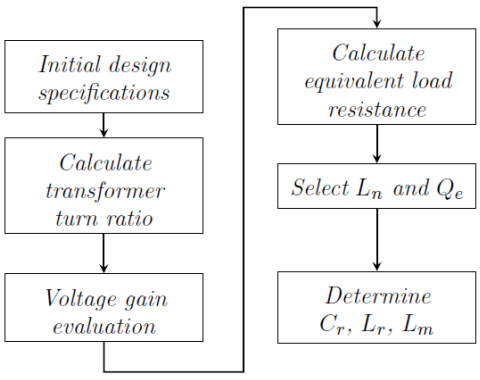

Fig. 8 The flowchart of design procedure

Table 1 Design parameters of topologies

Parameters	T1	T2	T3	T4
n	3	3	6	3
R_{ac} (Ω)	35.25	35.25	141	141
L_n	5	5	5	5
Q_e	0.56	0.56	0.56	0.56
C_r (nF)	82	88	20.15	22
L_r (uH)	33	34	125.6	131
L_m (uH)	165	170	628.4	655

Proportional-integral (PI) controller is used to obtain a constant output voltage against of input voltage and load variation. The switching pulses are generated and adjusted with PI controller. After testing the parameters of the simulated circuits, the controller parameters are selected as K_P is 0.04 and K_I is 3 for examined topologies.

Fig. 9 shows the resonant and magnetizing currents (I_r, I_{Lm}) in addition to the circulation of current in the diode rectifier at steady state for first topology. The current waveforms are divided into four process time. During the first process time $0.4 \leq t(s) < 0.400001$, the energy is transmitted to the secondary side of the transformer via primary side and between L_r and C_r the resonance occurs. There is a sinusoidal decrease in the negative direction of the resonant current I_r as well as linearly decrease in negative direction for the magnetizing currents I_{Lm} whereas the current in the primary side of the transformer equates to $I_r > I_{Lm}$. Additionally, the rectifier diodes D_1, D_2 conduct. Throughout the second process time between $0.400001 \leq t(s) < 0.4000045$, sinusoidal change occurs in the positive direction for I_r. Rectifier diodes D_1, D_2 are still conducting. The current in the primary side of the transformer can be expressed as $I_r > I_{Lm}$. The resonant frequency and the energy from the input is transported to the load. During the third process time $0.4000045 \leq t(s) < 0.400005$, the operation is similar with the first process only there is a sinusoidal increase in negative direction of I_r. During the fourth process time $0.400005 \leq t(s) < 0.40001$, the two transformers primary currents become zero and rise in the current of I_{Lm} and equates to the resonant current I_r. In this mode energy to the secondary side are no longer supplied by the primary side and the output filter capacitor C_0 supplies the load. With zero current switching D_1,

D_2 are naturally turned off and reverse recovery loss is eliminated.

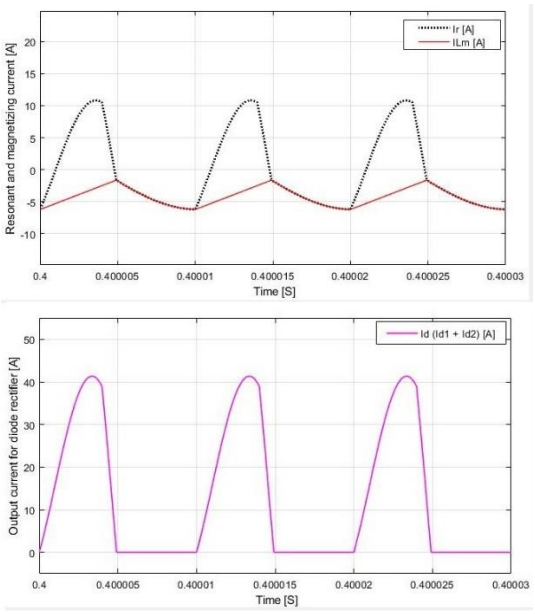

Fig. 9 Key waveforms of topology 1 at steady state

Fig. 10 shows the resonant and magnetizing currents (I_r, I_{Lm}) in addition to the circulation of current in the diode rectifier at steady state for second topology. The current waveforms are divided into four process time. The rectifier diodes D_1, D_4 conduct during the first and second process time and D_2, D_3 are on during the third and fourth process time. Occurrence of resonance between C_r and L_r while I_r and I_{Lm} decrease. Transformers primary current can be expressed as $I_r < I_{Lm}$. The variation in negative direction occurs for resonant current I_r at fourth process time. A linear change from positive direction to negative direction occurs for I_{Lm} and the energy is transferred to the secondary side from the primary side of the transformers.

Fig. 11 shows the resonant and magnetizing currents (I_r, I_{Lm}) in addition to the circulation of current in the diode rectifier at steady state for third topology. The current waveforms are divided into four process time which have the same performance as the first topology, but with some slight difference in the duration of the second and third and fourth process times.

Fig. 12 shows the resonant and magnetizing currents (I_r, I_{Lm}) in addition to the circulation of current in the diode rectifier at steady state for fourth topology. The current waveforms are divided into four process time which have the same performance as the second topology.

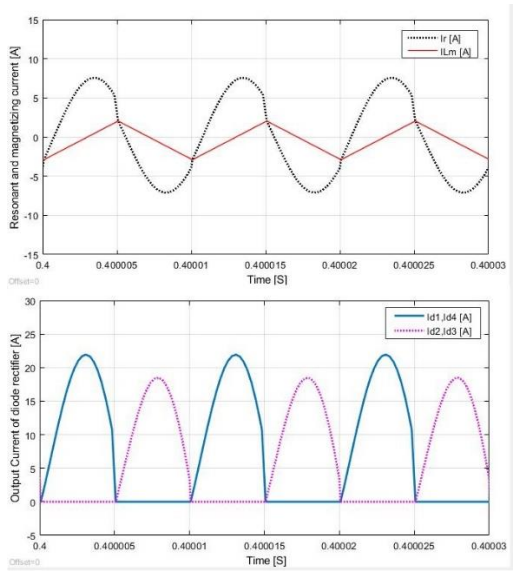

Fig. 10 Key waveforms of topology 2 at steady state

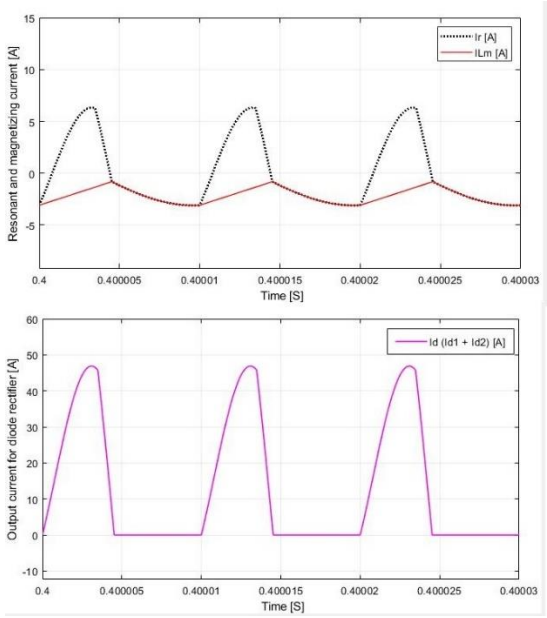

Fig. 11 Key waveforms of topology 3 at steady state

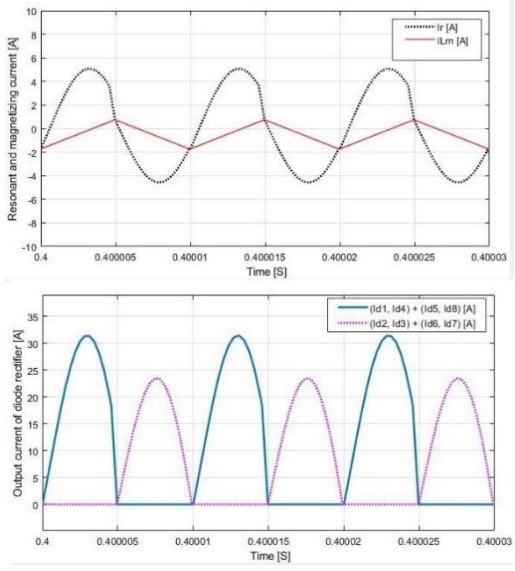

Fig. 12 Key waveforms of topology 4 at steady state

Fig. 13 shows the output power behaviour for examined topologies. The topologies reach to 645W, 712.9W, 681.1W, and 716.2W of output power at steady state taking based on calculated parameters, respectively. LLC resonant topologies with full-bridge rectifier have smoother output power because there is no transfer of energy to the secondary side of transformer at fourth process time.

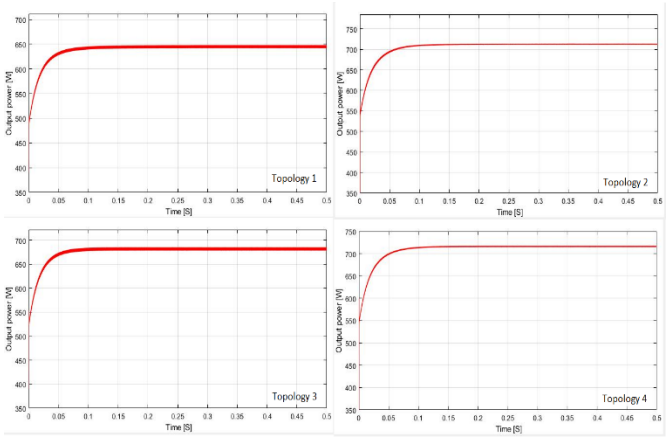

Fig. 13 Output power waveforms

For further comparison, each topology has been compared in terms of dynamic load variation from 100% to 65% load for the considered topologies at t = 0.2 sec then return it to 100% load at t = 0.3 sec. The dynamic response comparison is analyzed with output voltage and output current waveforms. The results are given in Fig. 14 for first and second topologies and Fig. 15 for third and fourth topologies. Whole presented topologies have similar behavior in terms of output voltage and output current. The output current for all considered topologies decreases by decreasing the load at t = 0.2 sec then increase by increasing the load at t = 0.3 sec.

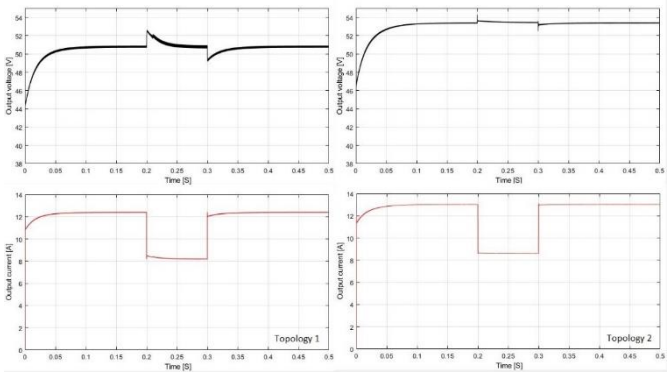

Fig. 14 Sudden load variation for first and second topologies

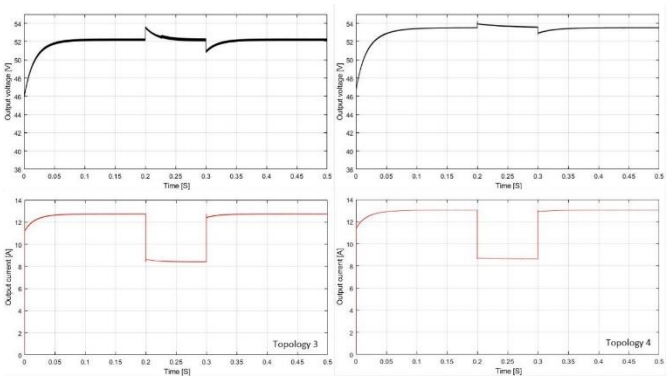

Fig. 15 Sudden load variation for third and fourth topologies

IV. DISCUSSION

The examined topologies have been compared in terms of efficiency. Table 2 shows input power, output voltage, current, and efficiency values for four considered topologies at full load. Furthermore, the efficiency values of each topology at full load are summarized in Fig. 14. It is obvious that the LLC resonant converters whose have full wave rectifier more efficient than the LLC resonant converters with full bridge rectifier due to the lowest conduction losses. First LLC converter topology achieves a slightly higher efficiency of 99% while fourth LLC converter topology achieves relatively less efficiency of 97.38%.

V. CONCLUSION

In this study, various topologies of LLC resonant converter using closed loop PI controller have been presented and was discussed in detail. The main improvement of this study is to compare most of the topologies used in the literature. Furthermore, the results present a guideline to select the proper topology and design details. After monitoring the output power of each design, it's clear that the LLC resonant half-bridge switching network with centre tapped full-wave rectifier is more efficient than the other topologies which achieves a high order of efficiency, reaching nearly 99% while the fourth LLC converter topology achieves a less efficiency, reaching nearly 97.38%. In addition, the output power for LLC resonant converters that have a full-bridge rectifier constituted from four diodes are smoother than those which have full-wave rectifier.

REFERENCES

[1] G.L. Kyriakopoulos, G. Arabatzis, "Electrical energy storage systems in electricity generation: Energy policies, innovative technologies, and regulatory regimes", Renewable and Sustainable Energy Reviews, Vol. 56, 2016, pp. 1044-1067, DOI: 10.1016/j.rser.2015.12.046.

[2] G. Arabatzis, G.L. Kyriakopoulos, P. Tsialis, "Typology of regional units based on RES plants: The case of Greece", Renewable and Sustainable Energy Reviews, Vol. 78, 2017, pp. 1424-1434, DOI: 10.1016/j.rser.2017.04.043.

[3] G. S. Sri, D. Subbulekshmi, "LLC resonant converter for battery charging application", International Journal of Electrical Engineering, Vol. 8 No. 4, 2015, pp. 379-388.

[4] H. Huang, "Designing an LLC resonant half-bridge power converter", Texas Instruments Power Supply Design Seminar, 2010, Texas Instruments: pp. 1-27.

[5] H. Choi, "Half-bridge LLC resonant converter design using FSFR-series Fairchild power switch", Fairchild Semiconductor Application Note AN-4151. 2007.

[6] X. Zhang, X. Wei, X. Wu, X. Yu, "Design of a digitally controlled full-bridge LLC resonant converter", NCCE 2018 International Conference on Network, Communication, Computer Engineering, 26-27 May 2018, Atlantis Press, Chongqing, China: pp. 978-984.

[7] M. Sharthi, R. Seyezhai, "A simple design and simulation of full bridge LLC resonant DC-DC converter for PV applications", Middle-East Journal of Scientific Research, Vol. 23 No. 2, 2015, pp. 285-292, DOI: 10.5829/idosi.mejsr.2015.23.02.22111

[8] C.C. Hua, Y.H. Fang, C.W. Lin, "LLC resonant converter for electric vehicle battery chargers", IET Power Electronics, Vol. 9 No. 12, 2016, pp. 2369-2376, DOI: 10.1049/iet-pel.2016.0066

[9] G.R. Prakash, J. Subramaniyan, M. Sivakumar, "Simulation and analysis of LLC resonant converter using closed Loop PI controller", International Journal of Advanced Engineering Research and Technology, Vol. 5 No. 1, 2017.

[10] N. Madhanakkumar, T.S. Sivakumaran, "Comparative study of closed loop control for resonant converter incorporating boost converter utilizing compression network", International Journal of Advanced Engineering Technology, Vol. 7 No. 2, 2016, pp. 85-92.

[11] K. Zheng, G. Zhang, D. Zhou, J. Li, S. Yin, "Modeling, dynamic analysis and control design of full-bridge LLC resonant converters with sliding-mode and PI control scheme", Journal of Power Electronics, Vol. 18 No. 3, 2018, pp. 766-777, DOI: 10.6113/JPE.2018.18.3.766.

[12] F. Kurokawa, K. Murata, "A new quick response digital modified PID control LLC resonant converter for DC power supply system", 2011 IEEE Ninth International Conference on Power Electronics and Drive Systems, 5-8 December 2011, IEEE, Singapore: pp. 35-39, DOI: 10.1109/PEDS.2011.6147220

[13] J. Jang, P.S. Kumar, D. Kim, B. Choi, "Average current-mode control for LLC series resonant dc-to-dc converters", 7th International Power Electronics and Motion Control Conference, 2-5 June 2012, IEEE, Harbin, China: pp. 923-930, DOI: 10.1109/IPEMC.2012.6258918

[14] J. Jang, M. Joung, S. Choi, Y. Choi, B. Choi, "Current mode control for LLC series resonant dc-to-dc converters", APEC 2011 Twenty-Sixth Annual IEEE Applied Power Electronics Conference and Exposition, 6-11 March 2011, IEEE, Fort Worth, TX, USA: pp. 21-27, DOI: 10.1109/APEC.2011.5744570

[15] J. Jang, M. Joung, B. Choi, H. Kim, "Dynamic analysis and control design of optocoupler-isolated LLC series resonant converters with wide input and load variations", 2009 IEEE Energy Conversion Congress and Exposition, 20-24 September 2009, IEEE, San Jose, CA, USA: pp. 758-765, DOI: 10.1109/ECCE.2009.5316558

[16] H. Ma, Q. Liu, J. Guo, "A sliding-mode control scheme for llc resonant DC/DC converter with fast transient response", IECON 2012 38th Annual Conference on IEEE Industrial Electronics Society, 25-28 October 2012, IEEE, Montreal, QC, Canada: pp. 162-167, DOI: 10.1109/IECON.2012.6388814

[17] T. Nishimura, Y. Adachi, Y. Ohta, K. Higuchi, E. Takegami, S. Tomioka, K. Jirasereemomkul, K. Chamnongthai, "Robust digital control for an LLC current-resonant DC-DC converter", Paper Presented at 2012 9th International Conference on Electrical Engineering/Electronics, Computer, Telecommunications and Information Technology, 16-18 May 2012, IEEE, Phetchaburi, Thailand, pp. 1-4, DOI: 10.1109/ECTICon.2012.6254168

[18] C. Buccella, C. Cecati, H. Latafat, K. Razi, "Comparative transient response analysis of LLC resonant converter controlled by adaptive PID and fuzzy logic controllers", IECON 2012 38th Annual Conference on IEEE Industrial Electronics Society, 25-28 October 2012, IEEE, Montreal, QC, Canada: pp. 4729-4734, DOI: 10.1109/IECON.2012.6389483